Comparison between rough and smooth plates within the same Rayleigh-Bénard cell

Jean-Christophe Tisserand, Mathieu Creyssels, Yoann Gasteuil, Hervé Pabiou, Mathieu Gibert, Bernard Castaing, Francesca Chillà

Comparison between rough and smooth plates within the same Rayleigh–Bénard cell

J.-C. Tisserand, M. Creyssels, Y. Gasteuil, H. Pabiou, M. Gibert et al.

Citation: Phys. Fluids **23**, 015105 (2011); doi: 10.1063/1.3540665
View online: http://dx.doi.org/10.1063/1.3540665
View Table of Contents: http://pof.aip.org/resource/1/PHFLE6/v23/i1
Published by the American Institute of Physics.

Comparison between rough and smooth plates within the same Rayleigh–Bénard cell

J.-C. Tisserand, M. Creyssels,[a] Y. Gasteuil, H. Pabiou, M. Gibert,[b]
B. Castaing, and F. Chillà[c]
Université de Lyon, ENS Lyon, CNRS, 46 Allée d'Italie, 69364 Lyon, Cedex 7, France

(Received 17 February 2010; accepted 30 November 2010; published online 20 January 2011)

In a Rayleigh–Bénard cell at high Rayleigh number, the bulk temperature is nearly uniform. The mean temperature gradient differs from zero only in the thin boundary layers close to the plates. Measuring this bulk temperature allows to separately determine the thermal impedance of each plate. In this work, the bottom plate is rough and the top plate is smooth; both interact with the same bulk flow. We compare them and address in particular the question whether the influence of roughness goes through a modification of the bulk flow. © *2011 American Institute of Physics*. [doi:10.1063/1.3540665]

I. INTRODUCTION

Understanding natural heat convection is of obvious practical interest. It also represents a very actual intellectual challenge, despite the apparent simplicity of its academic version, the Rayleigh–Bénard (RB) problem. The controversy in the past ten years around the high Rayleigh number behavior of RB cells[1–6] shows that the basic physical mechanisms of heat convection are not well understood.

In such a situation, tackling slightly different problems can shed new light on the main one. It is the purpose of the present paper, which explores the effect of a well defined roughness of a plate on the heat transfer between it and a fluid. Previous attempts give somewhat contradictory results.[7–11] We do not consider the work of Ciliberto *et al.*,[12] inspired by a proposition of Villermaux,[13] which shows that the absence of characteristic length in the roughness structure can modify the power law dependence of the Nusselt (Nu) versus the Rayleigh (Ra) number. Our work concentrates on well defined, regular, and periodic roughness.

At this stage, it is worth defining precisely the problem we consider. A Rayleigh–Bénard cell is a closed volume containing a fluid between two horizontal plates and vertical walls. With smooth boundaries, the control parameters are those defining the shape of the cell, as the aspect ratio $\Gamma = D/H$, where H is the height and D is the diameter of the cell, and two more specific ones, the Prandtl number Pr and the Rayleigh number Ra. $\mathrm{Pr} = \nu/\kappa$, where ν is the kinematic viscosity and κ, the heat diffusivity, is characteristic of the fluid.

$$\mathrm{Ra} = \frac{g\alpha\Delta T H^3}{\nu\kappa} \tag{1}$$

is the nondimensional measure of the temperature difference $\Delta T = T_h - T_c$ between the hot (T_h) and cold (T_c) plates. g is the gravitational acceleration and α the constant pressure thermal expansion coefficient. The thermal global response is given by the Nusselt number

$$\mathrm{Nu} = \frac{QH}{\lambda\Delta T}, \tag{2}$$

which compares the heat flux Q to the purely diffusive one $\lambda\Delta T/H$, where λ is the fluid thermal conductivity.

Several experiments[7–10] and a numerical simulation[11] examine the effect of the roughness of the plates on Nu. Shen *et al.*[7] and Du and Tong[8] use perpendicular triangular grooves to define square based pyramids on their plates. With 3 mm high pyramids, they observe a short cross-over when the thermal boundary layer height ($H/2\mathrm{Nu}$) matches the pyramids' one. For Rayleigh numbers under the crossover, the plate works as a smooth one. Above the cross-over, Nu is simply enhanced by a constant factor compared to the smooth case. With 9 mm high pyramids, they do not observe the cross-over, only the enhanced regime, by a factor significantly larger than that in the previous case. They observe systematic plumes at the tips of the pyramids. Qiu *et al.*[9] use the same pyramids, but sunk into the plate rather than glued. Either with 3 or 8 mm high pyramids, they observe the same power law $\mathrm{Nu} \propto \mathrm{Ra}^{0.35}$, with a higher prefactor in the 8 mm case.

In Ref. 10, linear triangular grooves are used. Matching the thermal boundary layer height with the grooves one occurs here at much higher Rayleigh number ($\mathrm{Ra} \simeq 10^{12}$ instead of $\mathrm{Ra} \simeq 10^{9}$ for Refs. 7 and 8) and they interpret the following regime ($\mathrm{Nu} \propto \mathrm{Ra}^{1/2}$) as the settlement of a turbulent thermal boundary layer.[14,15] Note that van den Berg *et al.*[16] obtain an equivalent result with a Taylor–Couette flow, whose equations are very similar to the Rayleigh–Bénard ones.

With a numerical simulation, Stringano *et al.*[11] also use linear triangular grooves. As in the experimental works,[7–10] a transition is observed toward an enhanced Nusselt regime when the thermal boundary layer height matches the grooves one. The behavior reported by Stringano *et al.*[11] for this regime is $\mathrm{Nu} \propto \mathrm{Ra}^{0.37}$ for the full three-dimensional calculation

[a]Also at Ecole Centrale de Lyon, CNRS, 36, avenue Guy de Collongue 69134 Ecully cedex, France.
[b]Also at MPI-DSO Bunsenstrasse 10, D-37073 Göttingen, Germany.
[c]Electronic mail: Francesca.Chilla@ens-lyon.fr.

and $\mathrm{Nu} \propto \mathrm{Ra}^{1/2}$ for the axisymmetric approximation, without any saturation up to the maximum Ra reached, implying a much wider cross-over than that in Ref. 7. However, Stevens *et al.*[17] suggest that the spatial resolution of this work is not high enough for large values of Ra, so that the calculated Nu is not accurate enough to pin down the scaling exponent. This argument does not hold for moderate Ra, just before the transition, and Stringano *et al.*[11] reported here a Nusselt surprisingly smaller than that for the smooth case.

Note that not only the height, but also the spatial period of the roughness could determine the thermal boundary layer thickness at the transition. However, with the kind of roughness used up to now, these two lengths are closely linked. It is why we choose here a different geometry which will allow us, in a future work, to explore these two influences.

The paper is organized as follows. In Sec. II, we present the apparatus, with particular emphasis on the differences with our previous works. In Sec. III, we present the results, both raw data and the various corrections we propose. The discussion and interpretation are given in Secs. IV and V. Before we conclude (Sec. VII), we present in Sec. VI hysteretic effects and long time relaxations associated with the transition observed.

II. EXPERIMENTAL SETUP AND MEASUREMENTS

The apparatus is basically similar to that described in Ref. 18. Our cell is cylindrical, $D=50$ cm in diameter. The wall is a stainless steel cylinder of thickness $e=2.5$ mm for two different heights: $H=1$ m (the tall one) or $H=0.2$ m (the small one). The plates are 3 cm thick. The top one is smooth made of copper and nickel plated. The bottom one is made of aluminium. Its roughness consists in a square array of square plots, $d=5$ mm of side and $h_o=2$ mm in height, with a period of $2d=1$ cm. The working fluid is de-ionized water, which is made free of gas *in situ* by boiling several hours under partial vacuum. The bottom plate has a heating wire, 13.55Ω, embedded as a spiral at the rear of this aluminium plate. It lies on a 2 cm thick isolating polytetrafluorethylene plate, which is supported by a 3 cm thick square aluminium table through eight hollow stainless steel feet. These feet go through a copper thermal screen which surrounds the whole cell. Heat leaks from the bottom plate are modelized by linear thermal links to the screen, the aluminium table, and the top plate (respectively, 0.7, 0.5, and 0.1 W/°C). Calibration of these links allows estimating the heat leaks within 0.5W.

The top plate is cooled through two counterflow spiral tubes, with 1 cm inner diameter, welded on the plate. Temperatures are measured through type K thermocouples. Three of them, including the control sensor, are on the top plate. Three other ones are on the bottom plate. One is stuck on the stainless steel wall to measure the bulk temperature T_b. Additional control platinum thermometers are glued on both plates. Eventual differences between measured temperatures in the same plate, which never go more than 3% of the total ΔT, are strictly proportional to the applied power. They can thus be attributed to heat conduction in the plates. For the measured Nu values, we use the sensors in the middle of the plates.

The water cooling the top plate is itself cooled through heat exchange with fresh water and temperature regulated via a 1 kW heater-cooler bath. To minimize uncontrolled heat leaks, the screen is regulated at the temperature of the middle of the cell (bulk temperature). The aluminium table is also temperature regulated.

Studies are made with water at various bulk temperatures from 25 (Pr=6.2) to 70 °C (Pr=2.5). This temperature is maintained constant for a series of experiments at various applied powers. This is the temperature chosen for the copper screen and for calculating the water physical properties.

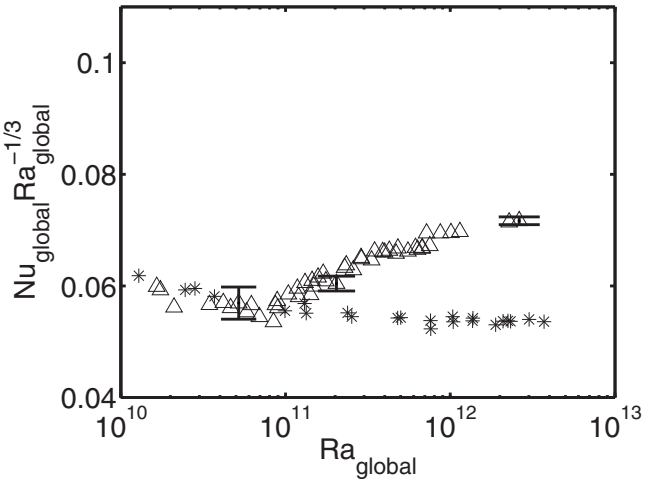

FIG. 1. The present global results are compared with previous results, obtained with two smooth plates, and the same wall. Open triangles: present work. Stars: symmetric smooth cell (Ref. 19). The shown error bars take into account our uncertainties on temperature and input power measurements.

III. RESULTS

In Fig. 1 we present our data.

$$\mathrm{Nu}_{\mathrm{global}} = \frac{QH}{\lambda(T_h - T_c)} \tag{3}$$

is presented in a compensated way $\mathrm{Nu}_{\mathrm{global}}\mathrm{Ra}_{\mathrm{global}}^{-1/3}$

$$\mathrm{Ra}_{\mathrm{global}} = \frac{g\alpha(T_h - T_c)H^3}{\nu\kappa} \tag{4}$$

to stress the differences with the smooth case. In the same figure, we plot the results of a previous work[19] using the same cell, but with both plates being smooth and made of copper (3 cm thick). It is clear that both sets of results are similar up to some threshold. After this threshold, the present results are above the previous ones. The depth of the thermal boundary layer at the threshold δ_{th} can be estimated as

$$\delta_{th} = \frac{H}{2\mathrm{Nu}_{\mathrm{global}}} \simeq 2 \text{ mm}, \tag{5}$$

which is the height of our square plots. We thus perfectly agree with previous works on this point.

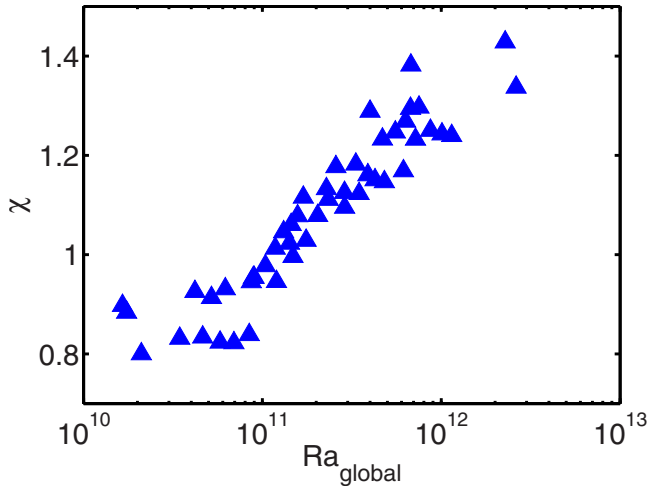

FIG. 2. (Color online) χ, the ratio between the temperature drops of the top and the bottom boundary layers, is plotted against the global Rayleigh number $\mathrm{Ra}_{\mathrm{global}}$.

The measure of the bulk temperature T_b, gives both (T_b-T_c), which is the temperature drop across the boundary layer of the smooth (top) plate, and (T_h-T_b), which is the temperature drop across the boundary layer of the rough (bottom) plate. With the same information, some authors[20–22] studied the asymmetric behavior of these plates. In their case, the asymmetry comes from the temperature dependence of the fluid properties. Here, it comes from the difference between the plates.

To quantify this asymmetry, they introduce the parameter χ

$$\chi = \frac{T_b - T_c}{T_h - T_b}, \tag{6}$$

which is 1 in the symmetric case. Our values for χ are shown in Fig. 2.

Above the threshold, χ is larger than 1 as expected. Note, however, that it is lower than 1 before the threshold. In the cited works,[20–22] the authors have no means to determine if the two boundary layers behave independently or if they mutually influence their behaviors through the bulk flow. Here, we can test this independency, as we know the behavior of a smooth plate.

If a symmetric cell has two independent smooth plates behaving the same as our top plate, the total temperature difference across this cell is $\Delta T_s=2(T_b-T_c)$. Its Nusselt number is

$$\mathrm{Nu}_s = \frac{QH}{\lambda \Delta T_s} \tag{7}$$

and its Rayleigh number is

$$\mathrm{Ra}_s = \frac{g\alpha \Delta T_s H^3}{\nu\kappa}. \tag{8}$$

We have to add a remark here. Measuring T_b with a single probe gives a more noisy and uncertain result than averaging on many probes all around the cell. Moreover, Brown and Ahlers[23] have shown that the large scale circulation (LSC) can sometimes be locked. This would result in an uncertainty in T_b-T_c and T_h-T_b equal to the temperature amplitude of the LSC, which can amount to 2%–8% of $\Delta T/2$.[24] While not significant for our larger values of χ, it could question our result that χ is smaller than 1 before the transition.

We have reasons, however, for arguing that our uncertainty cannot be so high. First, as will be seen later, our results for the smooth plate are in good agreement with previous ones, obtained in a symmetric cell.[19] Second, $\chi<1$ before the transition is confirmed with a second cell, also discussed in this work, with aspect ratio much larger (2.5) and thus a completely different LSC.

In Fig. 1, we show examples of error bars taking only account of our temperature and input power measurements uncertainty. Apart from a few points, they agree with the local dispersion of our results. The few exceptions could be due to systematic errors as discussed above or to the hysteretic behavior discussed in Sec. VI.

Similar to what we make for the top smooth plate, we can define a Nusselt number for the rough bottom plate

$$\mathrm{Nu}_r = \frac{QH}{\lambda \Delta T_r}, \tag{9}$$

with $\Delta T_r=2(T_h-T_b)$ and a Rayleigh number

$$\mathrm{Ra}_r = \frac{g\alpha \Delta T_r H^3}{\nu\kappa}. \tag{10}$$

As the ΔT can be different because of the asymmetry, a same run corresponds to different Ra values for the two plates. We thus prefer to use as the characteristic number

$$\mathrm{Ra}_* = \mathrm{RaNu} = \frac{g\alpha Q H^4}{\lambda \nu\kappa}, \tag{11}$$

which has the same value for both plates.

There are two reference behaviors for Nu versus Ra. The first one is $\mathrm{Nu}\propto \mathrm{Ra}^{1/3}$, which corresponds to a heat flux independent of the height H of the cell. That one is equivalent to $\mathrm{Nu}\propto \mathrm{Ra}_*^{1/4}$. The second one is $\mathrm{Nu}\propto \mathrm{Ra}^{1/2}$, corresponding to a heat flux independent of the dissipative coefficients (purely inertial convection). It is equivalent to $\mathrm{Nu}\propto \mathrm{Ra}_*^{1/3}$.

For clarity of the results, it will be interesting to define a reduced Nusselt

$${}^{\mathrm{red}}\mathrm{Nu} = \frac{\mathrm{Nu}}{\mathrm{Ra}^{1/3}} = \left(\frac{\mathrm{Nu}}{\mathrm{Ra}_*^{1/4}}\right)^{4/3}. \tag{12}$$

A purely inertial behavior gives a reduced Nusselt ${}^{\mathrm{red}}\mathrm{Nu}\propto \mathrm{Ra}_*^{1/9}$.

Tables I–III show part of our results (see Sec. VI for other results). Together with the raw data and the corresponding Nu for each plate, we give the corrected values corresponding to two effects. The first one is the finite conductivity of the wall, discussed in Ref. 25 or Ref. 26. The second one corresponds to the non-Oberbeck–Boussinesq (NOB) effects. We discuss them separately.

Roche *et al.*[25] propose an analytical formula for the correction of the wall conduction effect

TABLE I. Small cell results. Index s is for smooth and r is for rough. The two last columns are the corrected results.

Pr	Ra_*	Nu_s (raw)	Nu_r (raw)	Nu_s	Nu_r
4.49	4.60×10^{10}	66	70	62	65
4.34	9.60×10^{10}	76	88	71	84
4.32	1.94×10^{11}	87	110	83	105
4.34	3.85×10^{11}	101	136	97	130
4.33	5.33×10^{11}	108	148	104	142
6.19	4.96×10^{10}	64	70	60	66
6.19	4.91×10^{10}	63	70	59	66
6.10	2.55×10^{10}	56	57	52	53
6.12	1.27×10^{10}	48	48	45	44
6.20	5.02×10^{09}	39	39	36	36
6.19	6.29×10^{09}	42	40	38	37
2.46	4.38×10^{12}	190	274	186	264
2.46	3.82×10^{12}	184	264	180	255
2.46	3.82×10^{12}	184	261	180	252
2.46	3.27×10^{12}	178	250	173	242
2.50	2.67×10^{12}	169	235	164	227
2.49	1.61×10^{12}	151	202	146	195
2.49	8.58×10^{11}	130	168	125	162
2.49	4.27×10^{11}	111	137	106	132
2.49	2.12×10^{11}	95	110	91	105
2.53	1.04×10^{11}	83	87	78	83
2.49	4.10×10^{10}	65	67	61	63

TABLE II. Tall cell results for $T=40$ °C.

Pr	Ra_*	Nu_s (raw)	Nu_r (raw)	Nu_s	Nu_r
4.22	9.35×10^{13}	386	437	364	413
4.21	1.57×10^{14}	436	516	415	490
4.21	2.52×10^{14}	487	600	466	571
4.21	3.16×10^{14}	514	641	494	610
4.21	3.79×10^{14}	536	679	516	647
4.19	4.13×10^{14}	543	703	524	670
4.17	4.81×10^{14}	566	734	548	700
4.23	6.20×10^{13}	347	387	326	365
4.24	3.06×10^{13}	298	291	278	271
4.25	9.00×10^{12}	221	207	204	189
4.22	2.76×10^{12}	172	159	157	143
4.23	1.32×10^{12}	139	140	125	127
4.23	5.57×10^{13}	341	367	320	346
4.23	4.94×10^{13}	331	351	311	330
4.23	4.32×10^{13}	321	336	301	315
4.23	2.44×10^{13}	281	268	261	249
4.24	3.69×10^{13}	310	314	290	294
4.18	4.15×10^{14}	530	732	511	699
4.21	2.05×10^{14}	455	586	434	559
4.22	1.09×10^{14}	392	461	370	437
4.25	7.69×10^{13}	364	392	343	370
4.24	4.60×10^{13}	321	329	301	308
4.24	2.43×10^{13}	276	264	256	244
4.30	1.19×10^{13}	240	220	221	202
4.35	2.93×10^{12}	179	158	159	143
4.23	1.50×10^{13}	251	233	231	215

$$\mathrm{Nu}_{\mathrm{cor}} = \frac{\mathrm{Nu}_{\mathrm{measured}}}{1+f(W)}, \tag{13}$$

with

$$f(W) = \frac{A^2}{\Gamma \mathrm{Nu}}\left(\sqrt{1+\frac{2W\Gamma\mathrm{Nu}}{A^2}}-1\right) \simeq A\sqrt{2}\sqrt{\frac{W}{\Gamma\mathrm{Nu}}} \tag{14}$$

and $W=4\lambda_W e/\lambda D \simeq 0.5$, the ratio between the wall and the quiescent fluid heat conductances and $A \simeq 0.8$.

A warning must be raised, however. As explained in Ref. 25, this correction comes from a part of the heat power being directly injected in the bulk flow through the walls close to the plates, acting as an additional plate area. But this additional area is smooth. The extension of the correction to the case of a rough plate is not obvious. As a conservative approximation, we shall refer to the naive interpretation of roughness effects, as an enhancement factor S/S_o for the area of the plate (which is doubtful, however; see below). Within this interpretation, the ratio between the rough and smooth Nusselt numbers would be $(S/S_o)^{3/4}$ and the boundary layer on the rough plate would be thicker than that on the smooth one by a factor $(S/S_o)^{1/4}$. The relative corrections for the rough and smooth plates would be related as

$$\left(\frac{\delta\mathrm{Nu}}{\mathrm{Nu}}\right)_{\mathrm{rough}} = \left(\frac{\delta\mathrm{Nu}}{\mathrm{Nu}}\right)_{\mathrm{smooth}}\left(\frac{\mathrm{Nu}_{\mathrm{smooth}}}{\mathrm{Nu}_{\mathrm{rough}}}\right)^{7/6}. \tag{15}$$

The second correction comes from NOB effects and deserves a longer discussion.

NOB effects are extensively discussed for instance in Refs. 20–22. It appears from all these studies that the relative correction to the Nusselt number is second order in the temperature difference between the plates if the cell has symmetric plates. It would result in negligible (less than 1%) corrections with the temperature applied here. However, NOB effects result in a relative first order shift of the bulk temperature T_b from the mean temperature $T_m=(T_h+T_c)/2$. From the work of Ref. 20 the effect is often discussed in terms of the parameter χ

$$\chi = \frac{T_h - T_b}{T_b - T_c} = 1 - c_2\Delta T + \cdots \tag{16}$$

and thus

$$T_b - T_m = \frac{\Delta T}{2}\frac{1-\chi}{(1+\chi)} = c_2\left(\frac{\Delta T}{2}\right)^2 + \cdots. \tag{17}$$

Two theories attempted in calculating χ. References 20 and 22 start from the hypothesis that the hot (bottom, δ_h) and cold (top, δ_c) thermal boundary layer thicknesses are such that their characteristic temperatures

$$\theta_i = \frac{\nu_i\kappa_i}{g\alpha_i\delta_i^3} \tag{18}$$

are equal (the fluid properties are evaluated at the mean temperature of the boundary layer). While giving good agreement with some experiments, particularly for Nusselt corrections, this basic assumption has been proved to be wrong.[22]

TABLE III. Tall cell results for $T=70$ °C.

Pr	Ra_*	Nu_s (raw)	Nu_r (raw)	Nu_s	Nu_r
2.48	2.22×10^{15}	829	1184	809	1141
2.49	8.70×10^{14}	687	851	662	818
2.49	7.36×10^{14}	657	817	632	785
2.48	6.03×10^{14}	624	780	599	749
2.49	4.67×10^{14}	589	726	564	697
2.49	2.64×10^{14}	514	590	490	563
2.49	1.98×10^{14}	473	549	450	524
2.49	1.31×10^{14}	428	482	406	458
2.49	9.71×10^{13}	395	439	373	416
2.49	6.37×10^{13}	357	368	336	346
2.49	5.01×10^{13}	339	337	318	316
2.49	3.67×10^{13}	315	298	295	277
2.49	2.34×10^{13}	277	262	258	243
2.49	1.67×10^{13}	267	220	249	201
2.49	1.34×10^{13}	256	211	238	192
2.49	1.01×10^{13}	240	200	223	182
2.49	6.91×10^{12}	221	183	204	166
2.49	3.58×10^{12}	191	153	176	137
2.49	2.14×10^{13}	277	233	259	213
2.49	1.30×10^{14}	433	474	410	450
2.49	1.71×10^{14}	464	521	440	496
2.49	2.24×10^{14}	491	565	467	539
2.49	3.66×10^{14}	553	646	529	618
2.49	2.69×10^{15}	896	1197	876	1150

Ahlers *et al.*[22] propose to revisit thermal convection in a Blasius profile, taking into account the temperature dependence of fluid properties. They obtain χ without adjustable parameter and good agreement with their experimental results and those of Zhang *et al.*[21] However, they cannot propose an analytical formula and it is not clear if the Nusselt number obtained through their theory in Boussinesq conditions agrees with the observed one.

As we are concerned with linear corrections, the fluid being water, we can follow a different path. The theory of Ahlers *et al.*[22] shows well that at the linear level, the temperature dependence of α might have no influence. The only influent parameters are the temperature derivatives of ν and κ. In water, κ is nearly temperature independent. Dimensional considerations then yield to

$$c_2 = K(\mathrm{Pr})\frac{d\ln(\nu)}{dT}. \tag{19}$$

Indeed, K cannot depend on the other nondimensional parameter Ra, as it has to be independent of the height H of the cell, if the two plates behave independently. Ahlers *et al.*[22] propose two experimental values for c_2 at two different temperatures, thus different Pr: $T=29$ °C, Pr=5.53 and $T=40$ °C, Pr=4.34. Assuming a power law dependence of $K(\mathrm{Pr})$, we propose

$$c_2 = -0.061\mathrm{Pr}^{0.25}\left[\frac{d\ln(\nu)}{dT}\right]. \tag{20}$$

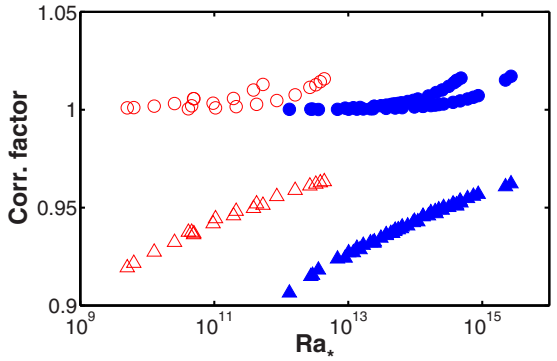

FIG. 3. (Color online) The correction factors used for the smooth plate's Nusselt number. Open symbols: small cell. Full symbols: tall cell. Circles: NOB corrections. Triangles: wall corrections.

This formula gives also reasonable agreement with the results of Ref. 21, in spite of the very large difference in the Prandtl number (Pr=2550 for glycerol).

Again, this correction is designed for smooth plates. However, we use the same formulas for rough plates. So, in both cases, the corrections for the rough plate are uncertain, except at low Ra_*, where the behaviors of both plates are similar. On the other hand, when different from the smooth one, the rough Nusselt number is much larger (see Sec. IV), making the corrections small.

Anyway, we use these corrections with two goals: first, to compare as finely as possible the smooth plate results with the traditional ones and second, to show that these corrections are small compared to the huge effects observed on the rough plate. Figure 3 resumes the applied factors for the Nusselt of the smooth plate.

Finally, we renounce to apply any correction for the finite heat conductivity of the plates. Indeed, in Ref. 27, such a correction is proposed based on the experimental comparison between various plates and a numerical simulation[28] gives some support for the existence of such a correction. However, contrary to previous corrections, we have no theory or model supporting the proposed formula. Moreover, in a recent work,[29] this correction proves to be inadequate, so we have no guarantee that such a correction would be meaningful in our case.

IV. DISCUSSION

The corrected values for the smooth plate are shown in Fig. 4 as $^{\mathrm{red}}\mathrm{Nu}_s=\mathrm{Nu}_s\mathrm{Ra}_s^{-1/3}$. They are in good agreement with previous measurements in the same cell, where both plates are smooth, shown as stars in the same figure. This agreement has many important consequences. It validates the usual approximation of two separate thermal resistances (the boundary layers), with a bulk between them approximately uniform in temperature. Certainly, the larger dispersion of the present results compared to the previous ones is partly due to some spatial variations of the bulk temperature, but this dispersion cannot hide the important trends. The small ($\Gamma=2.5$) and the tall ($\Gamma=0.5$) cell results nicely fit together, in agreement with previous observations on the poor influ-

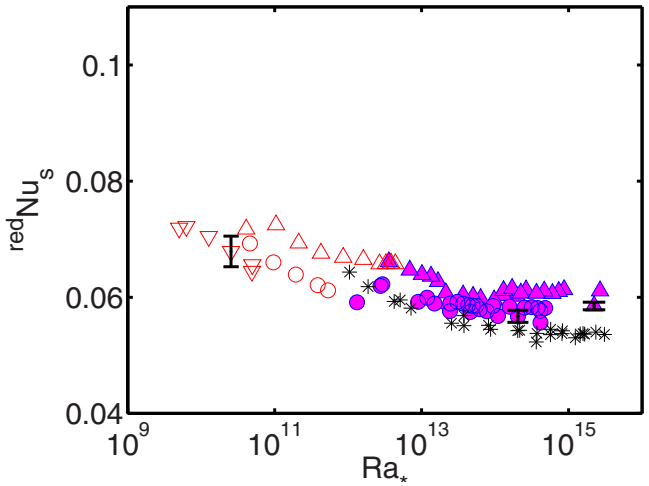

FIG. 4. (Color online) The reduced Nusselt number for the smooth plate. Open symbols: small cell. Full symbols: tall cell. Up triangles: $T=70$ °C, Pr=2.5. Circles: $T=40$ °C, Pr=4.3. Down triangles: $T=25$ °C, Pr=6.2. Stars correspond to a previous work with symmetric smooth plates (Ref. 19). The shown error bars take into account our uncertainties on temperature and input power measurements.

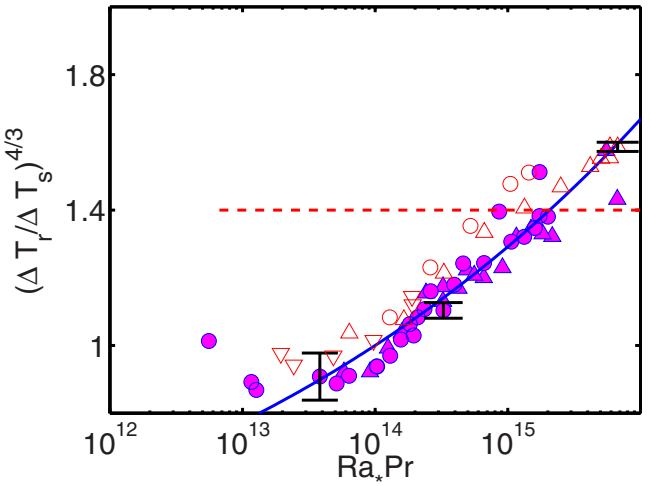

FIG. 6. (Color online) Ratio between the smooth and rough reduced Nusselts. The dashed line at 1.4 corresponds to the total area of the rough plate divided by the smooth one. The full line corresponds to a $(Ra_*Pr)^{1/9}$ behavior, i.e., the ratio between a $Nu \propto Ra^{1/2}$ one for the rough plate and $Nu \propto Ra^{1/3}$ for the smooth one. The shown error bars take into account our uncertainties on temperature measurements.

ence of the aspect ratio Γ.[30] The influence of the Prandtl number is clear, in reasonable agreement with previous studies.[31–34]

It is also clear that the present smooth plate results show no signature of the transition observed in the global results (see Fig. 1). It shows that the two boundary layers are independent of each other. This conclusion could not have been reached with a symmetric cell.

In contrast, the rough plate results (Fig. 5) show a clear transition when the thermal boundary layer approximately matches the height of the grooves. It corresponds to a different value of Ra_* for each set of data due to the different value of H in the tall cell (1 m) and in the small cell (20 cm). Note, however, as remarked in Sec. I, that we do not check the relative influence of the height and the period of the grooves.

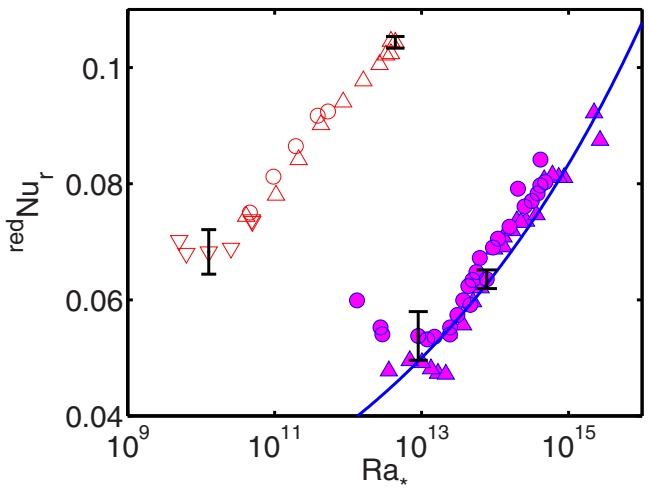

FIG. 5. (Color online) The reduced Nusselt number for the rough plate. The continuous line corresponds to $Nu \propto Ra^{1/2}$. Open symbols: small cell. Full symbols: tall cell. Up triangles: $T=70$ °C, Pr=2.5. Circles: $T=40$ °C, Pr=4.3. Down triangles: $T=25$ °C, Pr=6.2. The shown error bars take into account our uncertainties on temperature and input power measurements.

Before the transition, the Nusselt number is slightly reduced compared to the smooth case, as in Ref. 11. To qualify the behavior after the transition, we prefer to write: close to $Nu \propto Ra^{1/2}$ (or $Ra_*^{1/3}$), with no visible saturation. The comparison is shown in Fig. 5. The Ra interval is too small and our uncertainty too large for any significant *measure* of the exponent.

The comparison between the tall and small cells allows to finely check the eventual influence of the bulk flow. Indeed, reducing H by a factor of 5 lowers Ra by 125 and thus the Reynolds number by approximately 10.[35] For clarity, we present the results as the ratio between the rough and smooth reduced Nusselt (Fig. 6), which coincides with the ratio of the corresponding ΔT to the power $-4/3$, namely, $(\Delta T_s/\Delta T_r)^{4/3}$. It thus exactly represents the enhancement factor due to the roughness. As the abscissa, we take Ra_*, in the definition of which we use the tall cell height $H=1$ m. We multiply it by the Prandtl number Pr as we remark that it merges nicely the different temperatures. However, it well corresponds to our observed Prandtl dependence of the smooth plate Nusselt. So, this Pr factor should be interpreted as the rough plate Nusselt being Pr independent after the transition.

This plot confirms the previous analysis and shows that the enhancement factor is the same in both cells, tall and small. This, and the absence of any signature of the transition on the smooth plate, shows that the bulk flow has a negligible influence on the Nusselt number.

With our roughness profile, the contact area between the plate and the fluid is 1.4 larger than that with a smooth plate (1.4 is the area ratio). We see in Fig. 6 that the enhancement factor goes over this number without apparent saturation. An enhancement factor larger than the area ratio is also noticed in Ref. 8. However, they report a Nusselt behavior parallel to the smooth one, as if the enhancement reached a saturation. Indeed, as their grooves are 9 mm high rather

than $h_o=2$ mm for ours, their transition Ra_* value should be $(9/2)^4 \simeq 400$ times smaller than ours. The saturation can occur under their explored range, while being above ours.

V. INTERPRETATION

What could be the interpretation of our results? It seems clear that the total area enhancement, the area ratio, is not a good reference. If the ratio between rough and smooth Nusselt has to saturate, its value after saturation has to rely on a different basis.

Let us first examine the possibility that no saturation occur. This is indeed the interpretation of Roche *et al.*[10] for their experiment. They argue that the roughness of the plate fixes the size of the viscous sublayer of a turbulent thermal boundary layer, transforming the $\mathrm{Nu} \propto [\mathrm{Ra}/(\ln \mathrm{Ra})^3]^{1/2}$ behavior predicted by Kraichnan[14] in a pure $\mathrm{Nu} \propto \mathrm{Ra}^{1/2}$ one (note that the Pr dependence for the rough plate cannot be deduced from the Kraichnan work). However, they have the argument that a previous experiment in a similar cell,[35] with smooth plates, gives a behavior compatible with the Kraichnan one. Here, the smooth plate remains in the same regime, showing no trace of a transition to turbulence. Moreover, changing the height of the cell by a factor of 5 lowers the Reynolds number of the cell by a factor of 10 and that based on the height h_o of the roughness by a factor of 2. It has no influence on the behavior of the rough plate.

Despite the $\mathrm{Nu} \propto \mathrm{Ra}^{1/2}$ behavior, a transition to a turbulent state is thus improbable, while we cannot totally exclude it: some Taylor–Couette results[16] suggest that in the presence of boundary roughness, turbulence can occur for even smaller values of the Reynolds numbers than that of the small cell.

For an alternative explanation, we prefer to focus on the fact that part of the fluid, close to the plate, within the notches between the plots, cannot be taken by the flow and remain at rest until its buoyancy destabilization. Before this buoyancy destabilization, it thus reduces the heat exchange as it prevents the convection to go closer to the plate. After the buoyancy destabilization, on the opposite, it vigorously contributes to the heat exchange. This part, the shaded one in the Fig. 7, occupies a fraction σ of the plate. We shall call it the "sensitive area." Figure 7 suggests that $\sigma=1/4$. The rest of the plate contributes to the Nusselt number in the same way as that for the smooth plate. Thus, $\mathrm{Nu}_r=\sigma \mathrm{Nu}_{\mathrm{sens}} + (1-\sigma)\mathrm{Nu}_s$ and

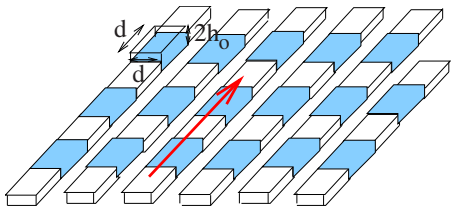

FIG. 7. (Color online) Schematic view of the rough plate. The shaded part is the fluid at rest, not washed by the flow (arrow). Also shown is the equivalent Rayleigh–Bénard cell whose buoyancy destabilization corresponds to the transition of the rough plate. $d=5$ mm is the half period of the roughness. $2h_o=4$ mm is twice the height of the notch.

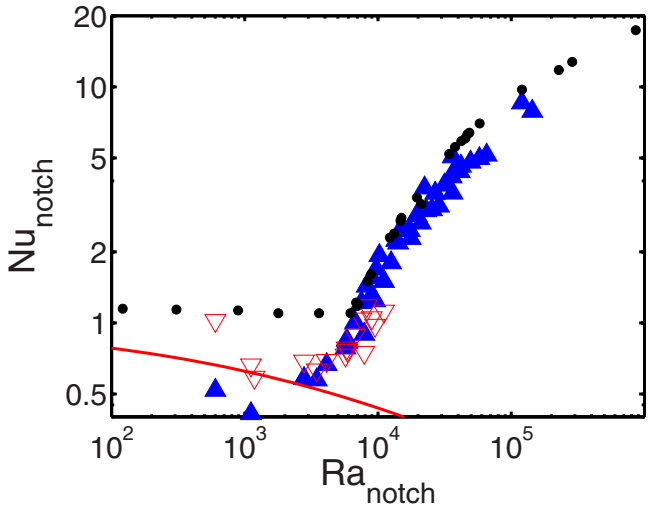

FIG. 8. (Color online) Effective Nusselt of the water between plots on the rough plate. Full triangles: small cell data, with proper height renormalization. Small black circles: data of Ref. 35 with renormalization of Ra to take account of the different aspect ratio (0.5 vs 1.25 here). Open triangles down: $2h_o\mathrm{Nu}_{\mathrm{sens}}/HN$. Continuous line: $1/(1+N)$, with $N=6\times10^{-2}\mathrm{Ra}_{\mathrm{notch}}^{1/3}$.

$$\mathrm{Nu}_{\mathrm{sens}} = \frac{1}{\sigma}\mathrm{Nu}_r - \left(\frac{1}{\sigma}-1\right)\mathrm{Nu}_s \simeq 4\mathrm{Nu}_r - 3\mathrm{Nu}_s. \tag{21}$$

We thus consider that $4\mathrm{Nu}_r-3\mathrm{Nu}_s$ gives us an experimental estimation of the heat conductivity of this sensitive area. We can compare it with our model in two separate cases, before and after the buoyancy destabilization of the fluid within the notch.

Such a destabilization is similar to that of a Rayleigh–Bénard cell of height $2h_o=4$ mm. The Rayleigh number $\mathrm{Ra}_{\mathrm{notch}}$ of such a cell is related to Ra_r as

$$\mathrm{Ra}_{\mathrm{notch}} = \frac{g\alpha\Delta T_r(2h_o)^3}{\nu\kappa} = \left(\frac{2h_o}{H}\right)^3 \mathrm{Ra}_r. \tag{22}$$

We thus expect this destabilization to occur for $\mathrm{Ra}_{\mathrm{notch}}$ being a few thousand, taking into account the limited aspect ratio of this cell: 5/4. Indeed, we obtain a critical value of $R_o \simeq 6\times10^3$ for $\mathrm{Ra}_{\mathrm{notch}}$, fairly coherent with this interpretation.

For $\mathrm{Ra}_{\mathrm{notch}} > R_o$, the heat conductivity of the notch should be similar to that of such a cell. We estimate the Nusselt number of the notch as

$$\mathrm{Nu}_{\mathrm{notch}} = \frac{2h_o}{H}\mathrm{Nu}_{\mathrm{sens}}. \tag{23}$$

Figure 8 compares the obtained experimental values for $\mathrm{Nu}_{\mathrm{notch}}$ to another experiment (full symbols), where the aspect ratio is even smaller (1/2).[35] The critical Rayleigh number of this experiment is thus larger (3×10^4) and we renormalize its Rayleigh numbers by a factor of 5 to fit with ours.

For $\mathrm{Ra}_{\mathrm{notch}} < R_o$, the quiescent fluid of height h_o should be topped with a smooth type boundary layer of height δ. The thermal conductivity of the sensitive area is thus equivalent to a layer of quiescent fluid, of total height $h_o+\delta$, and we can write

$$\mathrm{Nu}_{\mathrm{sens}} = \frac{H}{2(h_o+\delta)} = \frac{H}{2h_o}\frac{N}{1+N} \tag{24}$$

with $N=h_o/\delta$. To estimate δ, we take it equal to the boundary layer thickness on the adjacent areas, which behaves as a smooth plate. For such a smooth plate, according to the results of Fig. 4, $\mathrm{Nu}\simeq 6\times 10^{-2}\mathrm{Ra}^{1/3}$. Thus,

$$N = \frac{h_o}{\delta} = \frac{2h_o}{H}\frac{H}{2\delta} \simeq 6\times 10^{-2}\mathrm{Ra}_r^{1/3}\frac{2h_o}{H}$$
$$= 6\times 10^{-2}\mathrm{Ra}_{\mathrm{notch}}^{1/3}. \tag{25}$$

In Fig. 8, we compare $2h_o\mathrm{Nu}_{\mathrm{sens}}/HN$ and $1/(1+N)$ with $N=6\times 10^{-2}\mathrm{Ra}_{\mathrm{notch}}^{1/3}$ (open symbols). We clearly miss of low Ra data to be categoric, but the agreement is fair.

To conclude, the enhancement factor observed for the rough plate Nusselt compared to the smooth one is consistent with the buoyancy destabilization of the fluid captured inside the notches. This model not only justifies the general observation that the depth of the boundary layer fits the height of the plots at the transition, it also explains why the rough plate has a lower Nusselt than that of the smooth one just before the transition, as was previously observed by Stringano *et al.*[11] in their numerical simulation. The model also gives the right value of the enhancement factor after the transition. For much higher Ra_* number, it would predict that the rough plate comes back to the same Nusselt as that of the smooth one. However, in the mean range, a turbulent transition will probably occur.

Note that if this interpretation is correct, the $\mathrm{Ra}^{1/2}$ dependence of the rough plate Nusselt is fortuitous. Such a power law behavior cannot be predicted by our model.

VI. HYSTERESIS AND RELAXATION

In this section, we discuss some occurrences of hysteretic behavior of the rough plate, as for instance shown in Fig. 9.

In this example, the transition discussed in Sec. VI does not occur at the usual Ra_r value. Rather, when growing Ra_r by small steps, the rough plate continues in a $\mathrm{Nu}\propto\mathrm{Ra}^{1/3}$ mode, up to Ra_r values twice as large before raising its reduced Nusselt. Yet, instead of going to its equilibrium value within 1 h or so, the rough plate temperature slowly drops in a relaxation way during several days. We can follow such a relaxation during half a month, which is shown in Fig. 10. The applied power is 3300 W, corresponding to the highest Ra value at $T_b=70$ °C. The squares correspond to the evolution of $\Delta T_r=2(T_h-T_b)$. The triangles correspond to the evolution of $\Delta T_s=2(T_b-T_c)$. Their constant value shows that during all the relaxation of the rough plate, the smooth one keeps a constant Nusselt.

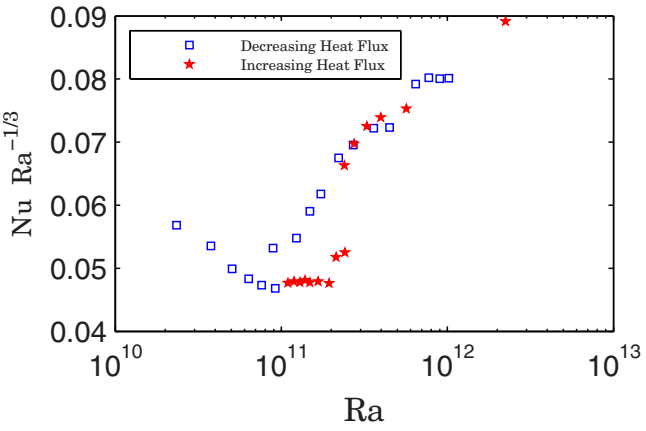

FIG. 9. (Color online) Hysteretic behavior of the rough plate for the tall cell. Stars: increasing Ra by small steps. Squares: decreasing Ra from its largest value.

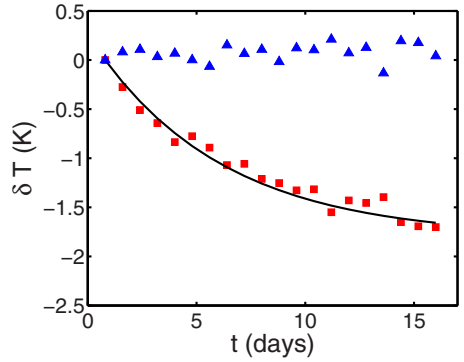

FIG. 10. (Color online) Time evolution of the plates temperatures compared to their initial one. Squares: rough plate. Triangles: smooth plate. Continuous line: exponential relaxation with time constant 6 days, and −1.8 °C of limit value.

The time dependence of ΔT_r better fit with an exponential function of time t, with time constant close to 6 days, than with a $\ln t$ behavior. A $\ln t$ behavior, corresponding to the absence of characteristic time, would have meant that the origin of the relaxation is in a complex system as the turbulent bulk flow itself. On the contrary, the origin has to be searched in a simple system.

Such observations can be interpreted in the frame of our model for the rough plate behavior. It would mean that maybe, depending on the orientation of the large scale flow, the bifurcation of the trapped quiescent fluid (shaded part in Fig. 7) to a convective state can turn to subcritical. Then, on some Ra range, each trapped part has a finite probability per unit time to become convective, resulting in an exponential relaxation of the global Nusselt number.

Note that we never observed such a hysteretic behavior with the small cell.

VII. CONCLUSION

The initial goal of this experiment is to look if the roughness of the plate can trigger the turbulence in the boundary layer. While not directly answering the question, our results give many interesting hints.

The Nusselt number of the top smooth plate is spectacularly similar to that obtained with two symmetric smooth plates. Its behavior seems insensitive to the transition experienced by the opposite rough plate. This is to be noted as, on the other hand, this behavior slightly differs from a pure $\mathrm{Ra}^{1/3}$ one, which means that the bulk flow has some influence on it. However, this result is consistent with many works (e.g., Ref. 36) showing the poor influence of the large

scale motion on the Nusselt number. Even those suggesting such an influence show that it is very tiny (close to 1%).[18]

Moreover, this work strongly corrects common intuitive feelings about the influence of roughness. At least close to the Rayleigh number where its effect appears, the increase in contact area with the fluid (the area ratio) is not a reference. The enhancement factor of the Nusselt number overcomes this limit without apparent saturation. If this saturation exists[8] and if the Nusselt number returns to a $\mathrm{Nu} \propto \mathrm{Ra}^{1/3}$ mode, the cross-over range is much larger than that suggested in Ref. 7. Our model, focusing on the destabilization of quiescent preserved fluid zones, has the advantage to capture most of the characteristics of the enhancement factor, including probably the hysteretic behavior.

If this interpretation is correct, the $\mathrm{Ra}^{1/2}$ behavior of the rough plate's Nusselt number Nu_r is fortuitous. A turbulent transition, which would more naturally explain it, is improbable. The main objection against it is that reducing the height of the cell by a factor of 5, and thus the Reynolds number based on the roughness size h_o by more than a factor 2, has no influence on this behavior. We cannot totally exclude it, however. The Taylor–Couette results[16] suggest that turbulence can occur for even smaller values of this Reynolds number. The final answer will come at larger values of the Rayleigh number based on h_o, by the occurrence or not of a saturation in $\mathrm{Nu}_r/\mathrm{Ra}_r^{1/3}$.

To resume, the independent behavior of both plates shows that the thermal exchange between a solid boundary and a fluid is largely a local process. However, the discrepancy between the Nusselt enhancement factor and the area ratio shows the limits of this locality. It shows how important is to understand the coherence of the flow along the plate.

ACKNOWLEDGMENTS

We thank M. Moulin and F. Vittoz for technical assistance. This work has been partly supported by the Agence Nationale pour la Recherche under Contract No. ANR-07-BLAN-0181.

[1] M. Sano, X. Z. Wu, and A. Libchaber, "Turbulence in helium-gas free-convection," Phys. Rev. A **40**, 6421 (1989).
[2] X. Chavanne, F. Chillà, B. Castaing, B. Hébral, B. Chabaud, and J. Chaussy, "Observation of the ultimate regime in Rayleigh-Bénard convection," Phys. Rev. Lett. **79**, 3648 (1997).
[3] J. J. Niemela, L. Skrbek, K. R. Sreenivasan, and R. J. Donnelly, "Turbulent convection at very high Rayleigh numbers," Nature (London) **404**, 837 (2000).
[4] J. J. Niemela and K. R. Sreenivasan, "Confined turbulent convection," J. Fluid Mech. **481**, 355 (2003).
[5] D. Funfschilling, E. Bodenschatz, and G. Ahlers, "Search for the "ultimate state" in turbulent Rayleigh-Bénard convection," Phys. Rev. Lett. **103**, 014503 (2009).
[6] G. Ahlers, S. Grossmann, and D. Lohse, "Heat transfer and large scale dynamics in turbulent Rayleigh-Bénard convection," Rev. Mod. Phys. **81**, 503 (2009).
[7] Y. Shen, P. Tong, and K. Q. Xia, "Turbulent convection over rough surfaces," Phys. Rev. Lett. **76**, 908 (1996).
[8] Y. B. Du and P. Tong, "Turbulent thermal convection in a cell with ordered rough boundaries," J. Fluid Mech. **407**, 57 (2000).
[9] X.-L. Qiu, K.-Q. Xia, and P. Tong, "Experimental study of velocity boundary layer near a rough conducting surface in turbulent natural convection," J. Turbul. **6**, N30 (2005).
[10] P. E. Roche, B. Castaing, B. Chabaud, and B. Hébral, "Observation of the 1/2 power law in Rayleigh-Bénard convection," Phys. Rev. E **63**, 045303 (2001).
[11] G. Stringano, G. Pascazio, and R. Verzicco, "Turbulent thermal convection over grooved plates," J. Fluid Mech. **557**, 307 (2006).
[12] S. Ciliberto and C. Laroche, "Random roughness of boundary increases the turbulent convection scaling exponent," Phys. Rev. Lett. **82**, 3998 (1999).
[13] E. Villermaux, "Transfer at rough sheared interfaces," Phys. Rev. Lett. **81**, 4859 (1998).
[14] R. H. Kraichnan, "Turbulent thermal convection at arbitrary Prandtl number," Phys. Fluids **5**, 1374 (1962).
[15] E. Siggia, "High Rayleigh number convection," Annu. Rev. Fluid Mech. **26**, 137 (1994).
[16] T. H. van den Berg, C. R. Doering, D. Lohse, and D. P. Lathrop, "Smooth and rough boundaries in turbulent Taylor-Couette flow," Phys. Rev. E **68**, 036307 (2003).
[17] R. J. A. M. Stevens, R. Verzicco, and D. Lohse, "Radial boundary layer structure and Nusselt number in Rayleigh-Benard convection," J. Fluid Mech. **643**, 495 (2010).
[18] F. Chillà, M. Rastello, S. Chaumat, and B. Castaing, "Long relaxation times and tilt sensitivity in Rayleigh Bénard turbulence," Eur. Phys. J. B **40**, 223 (2004).
[19] S. Chaumat, Ph.D. thesis, Ecole Normale Supérieure de Lyon, 2002 (unpublished).
[20] X. Z. Wu and A. Libchaber, "Non-Boussinesq effects in free thermal convection," Phys. Rev. A **43**, 2833 (1991).
[21] J. Zhang, S. Childress, and A. Libchaber, "Non-Boussinesq effect: Thermal convection with broken symmetry," Phys. Fluids **9**, 1034 (1997).
[22] G. Ahlers, E. Brown, F. Fontenele Araujo, D. Funfschilling, S. Grossmann, and D. Lohse, "Non-Oberbeck-Boussinesq effects in strongly turbulent Rayleigh-Bénard convection," J. Fluid Mech. **569**, 409 (2006).
[23] E. Brown and G. Ahlers, "Effect of the Earth's Coriolis force on the large-scale circulation of turbulent Rayleigh-Benard convection," Phys. Fluids **18**, 125108 (2006).
[24] E. Brown and G. Ahlers, "A model of diffusion in a potential well for the dynamics of the large-scale circulation in turbulent Rayleigh-Benard convection," Phys. Fluids **20**, 075101 (2008).
[25] P. E. Roche, B. Castaing, B. Chabaud, B. Hébral, and J. Sommeria, "Side wall effects in Rayleigh Bénard experiments," Eur. Phys. J. B **24**, 405 (2001).
[26] G. Ahlers, "Effect of sidewall conductance on heat-transport measurements for turbulent Rayleigh-Bénard convection," Phys. Rev. E **63**, 015303 (2000).
[27] E. Brown, A. Nikolaenko, D. Funfschilling, and G. Ahlers, "Heat transport in turbulent Rayleigh-Bénard convection: Effect of finite top- and bottom-plate conductivities," Phys. Fluids **17**, 075108 (2005).
[28] R. Verzicco, "Effects of nonperfect thermal sources in turbulent thermal convection," Phys. Fluids **16**, 1965 (2004).
[29] G. Ahlers, D. Funfschilling, and E. Bodenschatz, "Transitions in heat transport by turbulent convection at Rayleigh numbers up to 10^{15} ," New J. Phys. **11**, 123001 (2009).
[30] A. Nikolaenko, E. Brown, D. Funfschilling, and G. Ahlers, "Heat transport by turbulent Rayleigh-Bénard convection in cylindrical cells with aspect ratio one and less," J. Fluid Mech. **523**, 251 (2005); D. Funfschilling, E. Brown, A. Nikolaenko, and G. Ahlers, "Heat transport by turbulent Rayleigh-Bénard convection in cylindrical samples with aspect ratio one and larger," *ibid.* **536**, 145 (2005).
[31] G. Ahlers and X. Xu, "Prandtl-Number dependence of heat transport in turbulent Rayleigh-Bénard convection," Phys. Rev. Lett. **86**, 3320 (2001).
[32] P. E. Roche, B. Castaing, B. Chabaud, and B. Hébral, "Prandtl and Rayleigh numbers dependences in Rayleigh-Bénard convection," Europhys. Lett. **58**, 693 (2002).
[33] K. Q. Xia, S. Lam, and S. Q. Zhou, "Heat-Flux measurement in high-Prandtl-number turbulent Rayleigh-Bénard convection," Phys. Rev. Lett. **88**, 064501 (2002).
[34] S. Grossmann and D. Lohse, "Thermal convection for large Prandtl numbers," Phys. Rev. Lett. **86**, 3316 (2001); "Fluctuations in Rayleigh-Bénard convection: The role of plumes," Phys. Fluids **16**, 4462 (2004).
[35] X. Chavanne, F. Chillà, B. Chabaud, B. Castaing, and B. Hébral, "Turbulent Rayleigh-Bénard convection in gaseous and liquid He," Phys. Fluids **13**, 1300 (2001).
[36] S. Ciliberto, S. Cioni, and C. Laroche, "Large-scale flow properties of turbulent thermal convection," Phys. Rev. E **54**, R5901 (1996).